ACS APPLIED MATERIALS & INTERFACES

Research Article

www.acsami.org

Uniaxially Stretched Flexible Surface Plasmon Resonance Film for Versatile Surface Enhanced Raman Scattering Diagnostics

Kaichen Xu,[†,∥,‡] Zuyong Wang,[#,‡] Chuan Fu Tan,[†] Ning Kang,[⊥] Lianwei Chen,[†] Lei Ren,[⊥] Eng San Thian,[§] Ghim Wei Ho,[†] Rong Ji,[*,∥] and Minghui Hong[*,†]

[†]Department of Electrical and Computer Engineering, National University of Singapore, 4 Engineering Drive 3, 117576, Singapore
[∥]Data Storage Institute, (A*STAR) Agency for Science Technology and Research, 2 Fusionopolis Way, 138634, Singapore
[§]Department of Mechanical Engineering, National University of Singapore, 9 Engineering Drive 1, Singapore 117576, Singapore
[⊥]Department of Biomaterials, College of Materials, Xiamen University, Xiamen, 361005, China
[#]College of Materials Science and Engineering, Hunan University, Changsha, 410082, China

Supporting Information

ABSTRACT: Surface-enhanced Raman scattering (SERS) spectroscopy affords a rapid, highly sensitive, and nondestructive approach for label-free and fingerprint diagnosis of a wide range of chemicals. It is of great significance to develop large-area, uniform, and environmentally friendly SERS substrates for in situ identification of analytes on complex topological surfaces. In this work, we demonstrate a biodegradable flexible SERS film via irreversibly and longitudinally stretching metal deposited biocompatible poly(ε-caprolactone) film. This composite film after stretching shows surprising phenomena: three-dimensional and periodic wave-shaped microribbons array embedded with a high density of nanogaps functioning as hot-spots at an average gap size of 20 nm and nanogrooves array along the stretching direction. The stretched polymer surface plasmon resonance film gives rise to more than 10 times signal enhancement in comparison with that of the unstretched composite film. Furthermore, the SERS signals with high uniformity exhibit good temperature stability. The polymer SPR film with excellent flexibility and transparency can be conformally attached onto arbitrary nonplanar surfaces for in situ detection of various chemicals. Our results pave a new way for next-generation flexible SERS detection means, as well as enabling its huge potentials toward green wearable devices for point-of-care diagnostics.

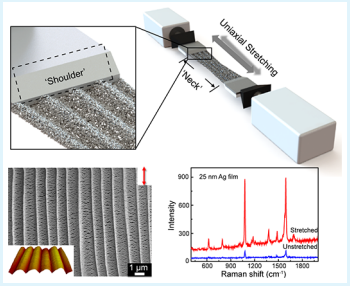

KEYWORDS: *surface-enhanced Raman scattering, biodegradable flexible film, irreversibly stretching, wave-shaped microribbons, nanogrooves array*

INTRODUCTION

Flexible wearable sensors have been envisioned as promising diagnostic tools owing to their considerable applications in healthcare,[1,2] protective equipment inspection,[3] environmental monitoring,[4] and homeland security.[5] In particular, to develop biocompatible and environmentally friendly biosensors is of paramount importance for their potential applications in wearable and point-of-care (POC) diagnostics to eliminate waste streams.[6−8] Such biosensors built with biodegradable and biocompatible materials as backbone features can be integrated into living tissues as well as portable spectrometers for therapeutic and diagnostical purposes.[8,9] Among a variety of biosensors, surface-enhanced Raman scattering (SERS), an accurate label-free and fingerprint detection means, is emerging as one of the most cutting-edge techniques for noninvasively tracing extremely low-concentration molecules.[10] Primarily based on localized surface plasmon resonances (LSPRs), SERS is capable of enhancing excited photons as well as vibrational scattering of analytic molecules via the amplification of electromagnetic (EM) fields, which relies on localizing light into the nanoscale volumes.[11,12] Although tremendous advances have been made in demonstrating a plenty of SERS substrates with sub-10 nm gap structures to allow the identification of fingerprint information on probe molecules adsorbed on plasmonic nanostructures, most traditional approaches either based on chemical syntheses or complex lithographic routes, such as focused ion beam and electron beam lithography, suffer from nonuniformity or low-throughput issues.[13,14]

Furthermore, conventional SERS substrates employ rigid materials without biodegradability, such as glass and silicon as building blocks, which require to extract objective analytes and then be adsorbed onto the hard plasmonic templates for detection.[15] In order to satisfy the requirement of increasingly demanded POC diagnostics for nonlaboratory settings' monitoring, the in situ detection approach is more preferred for practical applications, where the SERS substrates are directly attached onto the sample surfaces of interest.[16] However, due to the lack of flexibility, the rigid SERS substrates have poor conformal contact with objects, especially those with

Received: May 11, 2017
Accepted: July 13, 2017
Published: July 13, 2017

DOI: 10.1021/acsami.7b06669
ACS Appl. Mater. Interfaces 2017, 9, 26341−26349

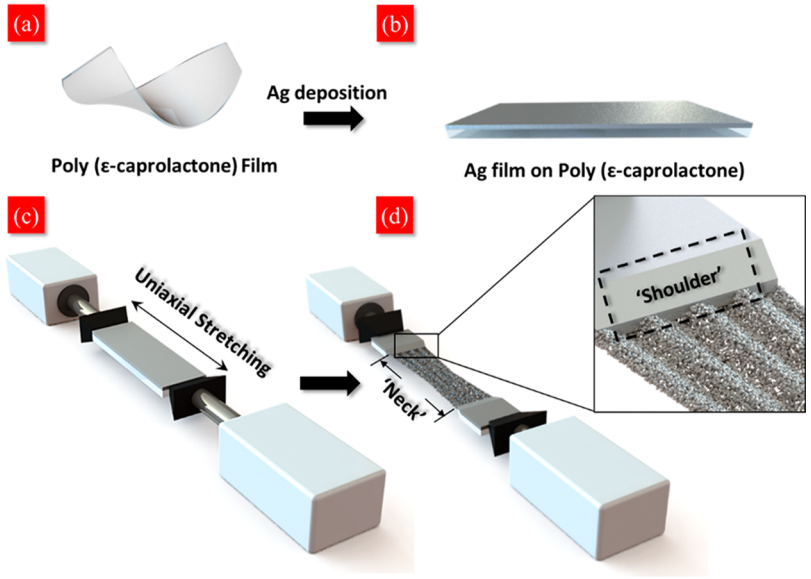

Figure 1. Schematic diagram of stretching polymer SPR film under an external mechanic force. (a) Flexible PCL polymer film. (b) Ag film is deposited on PCL polymer film by an electron-beam evaporator. (c) The polymer SPR film is fixed onto a mechanical machine. (d) The uniaxial stretching of polymer SPR film at a constant stretching speed. Two primary characteristics are observed: neck formation and shoulder propagation. The inset highlights the nanostructures' formation in the neck region.

complex topological shapes. On the other hand, because of the demand to excitate incident photons and then collect Raman signals from the back side of the SERS substrates for in situ detection, high transparency of flexible substrates needs to be achieved.[17]

To overcome these challenges, we develop a new biocompatible and biodegradable SERS substrate via irreversibly and uniaxially stretching metal deposited flexible poly(ε-caprolactone) (PCL) surface plasmon resonance (SPR) film as wearable sensors for in situ detection of analytes. This approach has several advantages in practical SERS applications for the following reasons.

First, the PCL film, as an excellent flexible, biodegradable and biocompatible material with good transparency (~90%) and temperature stability (9.62%), is for the first time employed as a building block for flexible SERS substrates. Until now, numerous materials, such as adhesive tape,[18,19] filter paper,[17,20] and polymers,[21−27] have been applied as frameworks of the flexible SERS substrates. The "paste and peel off" concept based on commercial tape represents a simple and viable approach for efficient extraction of analytes on arbitrary surfaces, but the uniformity of the plasmonic structures is not well considered and most importantly, the adhesive tape is a nonbiodegradable material, which violates the goal for environmental protection and sustainability.[18,19] Although the paper-based SERS substrates with biodegradability are economical and storable, their opaqueness property prevents the collection of SERS signals from the opposite surface.[17,20] Recently, flexible and tunable SERS substrates have attracted intense research attention, which are based on stretchable materials, such as polydimethylsiloxane (PDMS).[21−24,28,29] Relying on their elastic deformation property, it is possible to actively control the nanogap distance between metallic nanoparticles on their elastic and stretchable polymer films, which enables the effective detection of large biomolecules and reversible plasmonic spectral shifts.[21,22,24] However, it faces formidable challenges to exactly control the optical properties of plasmonic film and uniformity of hot-spots under an external strain to reversibly deform the substrate in practical applications. Depending on the irreversible transformation of ductile polymer film, the stretching of the composite film is studied.[30,31] However, how to realize the polymer-based homogeneous nanostructures that can be massively reproduced still remains an enormous challenge.

Second, the uniaxial stretching of Ag/PCL composite film results in the formation of large-area periodical microribbons with a high density of plasmonic nanogaps and V-shaped nanogrooves, which can be tuned via flexibly varying the thickness of metallic film. These plasmonic nanogaps and nanogrooves confine incident light in the form of near-field evanescent waves, serving as hot-spots to enhance SERS signals. Compared to conventional methodologies to achieve nanogaps that rely on several complex and precise fabrication procedures, our approach makes use of plastic strain to induce increased distances between adjacent lamellae within PCL crystals to create a plenty of plasmonic nanogaps. Furthermore, different from traditional methods, which apply FIB milling, photolithography coupled with anisotropic etching or elastomeric materials to achieve V-shaped groove profiles,[32−35] this approach affords a new route to produce periodical V-shaped nanogrooves array along the elongation direction via laterally shrinking PCL crystals.

Third, the ultrathin (~10 μm) polymer SPR film can be intimately attached onto arbitrary topological surfaces for in situ detection of analytes for POC diagnostics because of their high transparency and flexibility. The features of low-cost, biodegradability, and batch-fabrication of the polymer SPR film open great opportunities to integrate the novel flexible SERS substrates with portable Raman spectrometers in the applications of resource-limited settings. Furthermore, the stretching induced plasmonic nanostructures presents good temperature stability (9.62%) and uniformity (6.48%) of the detected SERS signals. This new stretched polymer SPR film provides great potentials to construct next-generation wearable sensors.

DOI: 10.1021/acsami.7b06669
ACS Appl. Mater. Interfaces 2017, 9, 26341−26349

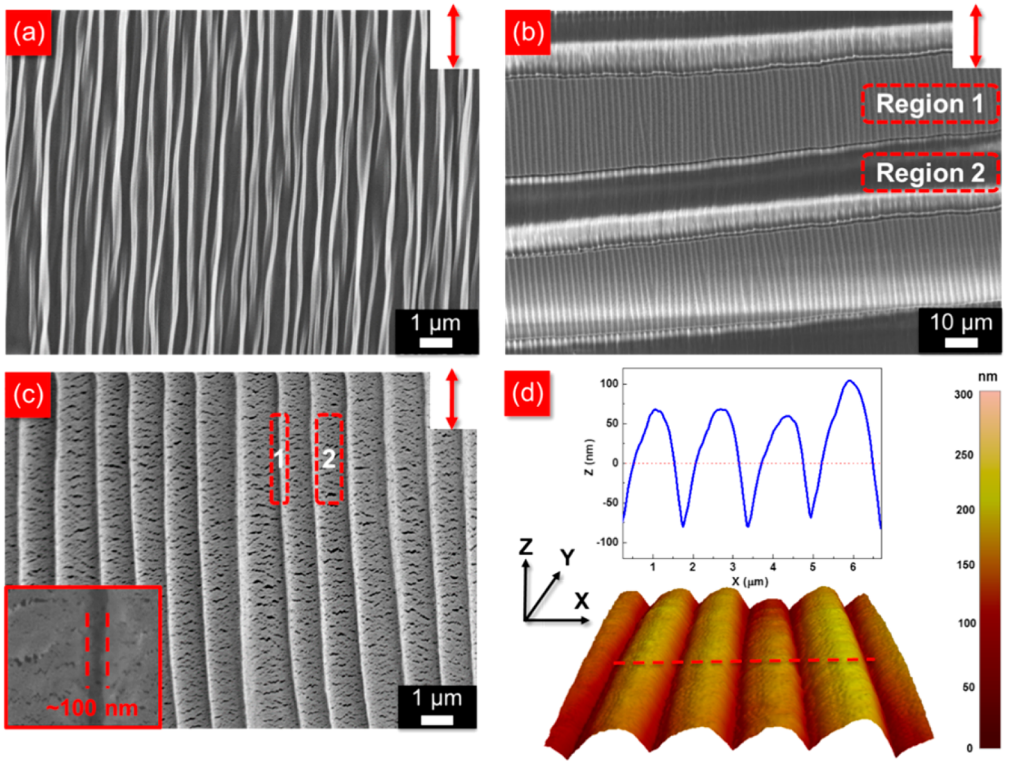

Figure 2. Surface morphology of stretched polymer SPR film without (a) and with (b–c) 25 nm Ag film. The arrows denote the direction of externally applied stress. The polymer SPR film at a width of 4 cm is drawn from 4 cm (initial length) to 10 cm (stretched length). The inset in panel c shows the dimension of the nanogroove. The dashed boxes in panel c indicate the nanogroove (1) and nanogaps (2), respectively. (d) Morphologies of four complete periods of polymer SPR film demonstrate 3D wave-shaped structures. The inset in panel d illustrates line scanning obtained across the dashed line.

RESULTS AND DISCUSSION

To develop a high-performance flexible SERS biosensor, it is crucial to produce high density of hot-spots on the substrate. First, a flexible PCL film at a length of 9 cm, width 4 cm and thickness around 20 μm is deposited with silver (Ag) film by an electron-beam evaporator as illustrated in Figure 1a,b. After fixing the polymer SPR film onto a mechanical machine for stretching, the efficient dimension of polymer SPR film is set as 4 cm (Figure 1c). The Ag decorated PCL polymer film is then subjected to uniaxial stretching from 4 to 10 cm under a constant velocity. Upon the stretching, the ductile polymer SPR film first goes through a few percent (~10%) of homogeneous uniaxial extension, followed by the formation of localized "neck" due to the mechanical instability of the polymer film. The neck region gradually expands and propagates via the spread of "shoulder" from the deformed region (neck region) to undeformed region until the polymer SPR film is entirely stretched (Figure 1d). This procedure involves plastic deformation, longitudinal elongation, transverse dimension's reduction as well as the thinning of the polymer SPR film. During the stretching, the deformation of the polymer SPR film gives rise to the formation of massive tiny cracks inside the brittle Ag film. These cracks are expected to serve as hot-spots to boost SERS signals. After the stretching, the thickness of the polymer SPR film evolves from ~20 to ~10 μm.

To untangle the surface morphology of the stretched polymer SPR film, first, the uniaxial stretched PCL polymer film is characterized by a scanning electron microscope (SEM). As can be seen in Figure 2a, the uniaxially stretched PCL films are comprised of many highly oriented nanoridges and nanogrooves along the stretching direction, which are not observed on the unstretched PCL films (Figure S1a and c). It is worthwhile to note that compared with the unstretched polymer film, the stretched PCL polymer film exhibits a higher transmittance (~90%), which promotes strong Raman excitation via laser interacting with the detected molecules to enhance Raman signals' intensity (Figure S2a). After depositing a layer of Ag film at a thickness of 25 nm, the polymer SPR film after the same stretching allows the formation of periodically plasmonic microribbons perpendicularly to the elongation direction (region 1), while the area of inter-ribbons is only composed of PCL polymer film (region 2) (Figure 2b). This observation is also verified by chemical elemental mapping with energy-dispersive X-ray (EDX) spectroscopy (Figure S3a–c). In the SPR effective region with metallic hot-spots, we observed very unique phenomena as shown in Figure 2c. To be specific, a new type of large-area microribbons array parallel to the stretching orientation at a period of ~1 μm is formed. On the ribbons, plenty of transgranular nanogaps are created at a dimension of tens of nanometers. Among neighboring ribbons, there are many nanogrooves at a width of ~100 nm along the stretching axis. The EDX analyses indicate the distribution of Ag nanostructures on the polymer SPR film after the stretching (Figure S3d). In order to further reveal the surface morphology of the stretched polymer SPR film, an atomic force microscope (AFM) is applied to further characterize the sample surface. It can be seen from Figure 2d that microribbons array demonstrates well-defined three-dimensional (3D) wave-shaped geometry at an average height of ~110 nm. Among these nanoribbons, there are various nanoislands being created, also indicating that the stretching of polymer SPR film

DOI: 10.1021/acsami.7b06669
ACS Appl. Mater. Interfaces 2017, 9, 26341–26349

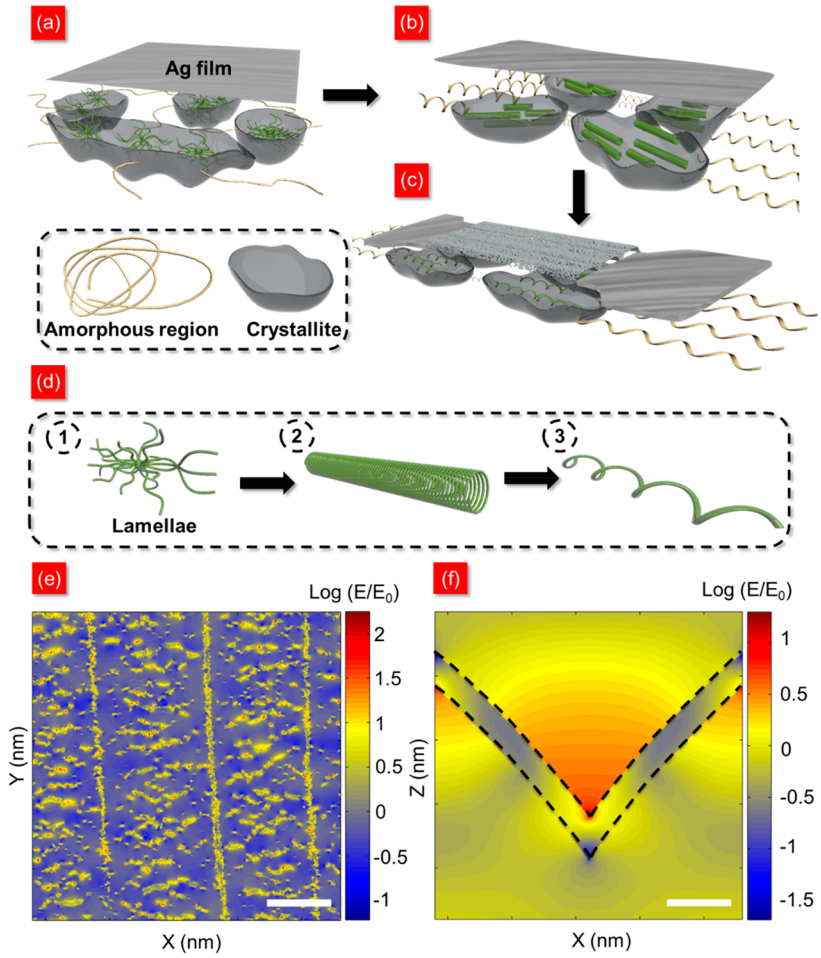

Figure 3. (a–c) Proposed models of nanostructures' formation via stretching polymer SPR film. The evolution of lamellae in panels a–c is highlighted in panel d, respectively. The PCL polymer film is composed of crystallitic and amorphous phases. There are multilayered lamellae in the crystallitic phases. Calculated electric field distributions of the microribbons (scale bar = 500 nm) (x–y plane) (e) and nanogrooves (scale bar = 50 nm) (x–z plane) (f).

contributes to the formation of many Ag nanogaps (Figure S1d). Meanwhile, we also carry out similar experiments to demonstrate the structures' formation of other three metal materials, including Ni, Al, and Au at a thickness of 25 nm, deposited on PCL polymer films after the stretching, the morphology of which are probably associated with brittleness and ductility of metals (Figure S4). In particular, Au, as one of the most frequently used materials for excellent plasmonic performance, can form similar nanostructures like Ag. However, the nanogaps' size of Au (average 10 nm) is a bit smaller than that of Ag (average 20 nm) at the same thickness, which is attributed to the higher ductility of gold beings able to withstand a larger elongation.

It is of great interest to gain insight into the mechanisms of nanostructures' formation on semicrystalline PCL polymer films, which are composed of crystallitic and amorphous phases (Figure 3a). Upon applying a uniaxial stress, the crystallite and amorphous regions present an excellent tendency to orient along the stretching direction (Figure 3b). After the yield strength, the dual-layered polymer SPR film after the stretching forms plentiful tiny cracks on the superficial Ag nanoparticle layer, while the beneath PCL layer remains intact integrity, because of a significant difference in the ductilities of the metal thin film and polymer substrate. However, a continuous stretching leads to plastic deformation of the PCL layer, accounting for the observed formation of two distinct regions: PCL monolayer and Ag/PCL dual layers (Figure S5a). The further increase of the plastic strain on the PCL monolayer results in a force propagating to the Ag/PCL dual layers and reorientation of the PCL crystals in these regions along the elongation direction. The PCL crystals further occur a plastic strain following to its Poisson's ratio, which results in lateral shrinkage and increased distance among adjacent lamellae within a crystal (Figure 3c and d). Such deformation of PCL crystals accounts for the observed formation of nanogrooves along stretching direction and transgranular nanogaps in the superficial Ag layer, respectively. After the polymer SPR film is entirely deformed, the continued stretching of the polymer SPR film gives rise to the splitting of Ag/PCL region because of the strain of PCL monolayer region to be near the break point and insufficient to support the sustained elongation of the polymer SPR film (Figure S5b). Moreover, our further stretching of the polymer SPR film initiates the Ag film to debond from the beneath PCL polymer film because of the larger tractions on the interface (Figure S5f).[36] Our experiment also finds that Ag film thicker than 25 nm is difficult to form nanogrooves and nanogaps, which are ascribed to the larger bending resistance of the thicker Ag film.

To further reveal the optical properties of the polymer SPR film and identify the nature of the formation of hot-spots, finite-

DOI: 10.1021/acsami.7b06669
ACS Appl. Mater. Interfaces 2017, 9, 26341–26349

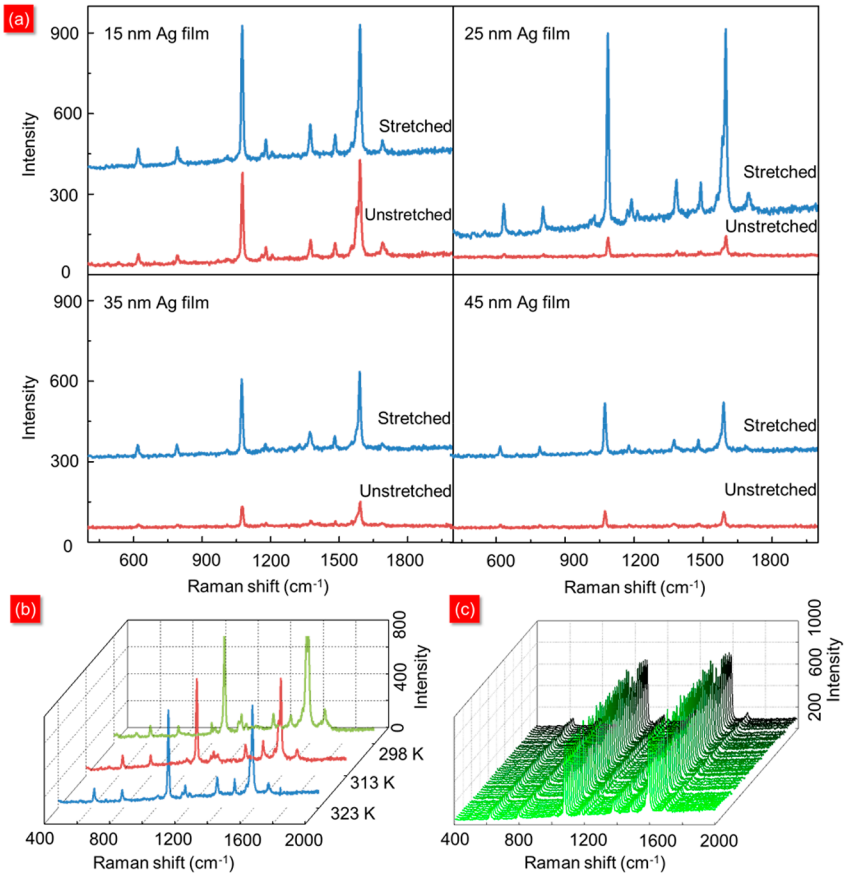

Figure 4. (a) SERS spectra of 4-MBT molecules adsorbed on polymer SPR film with different thicknesses of Ag films before and after the stretching. (b) Temperature stability characterization of SPR polymer film. During the stretching, the environmental temperature is elevated from room temperature (298 K) to 323 K. (c) SERS spectra of 4-MBT molecules from 45 random points on the polymer SPR film. The polymer SPR film at a Ag thickness of 25 nm is stretched from 4 to 10 cm. All the SERS spectra are obtained at the laser excitation wavelength of 514 nm, power 0.15 mW, acquisition time 10 s, and accumulation time 1.

difference-time-domain (FDTD) simulation is applied to investigate the distributions of near-field electromagnetic fields. Figure 3e depicts two-dimensional (2D) electric field intensity distribution (Log scale) of the stretched polymer SPR film at the Ag film's thickness of 25 nm in the region of microribbons in Cartesian $x-y$ plane at the excitation wavelength of 514 nm. The incident light is polarized along the stretching axis. The nanogaps resemble nanocavities to converge the incident photons, resulting in higher electromagnetic enhancement. The average simulated electric field intensity (E/E_0) is found to be ~18. Meanwhile, V-shaped nanogrooves also act as plasmonic nanocavities, which can strongly focus incident electromagnetic wave into nanoscale gaps located at the groove tips under normal illumination in $x-z$ plane, where the polarization of excitation light is perpendicular to the stretching direction (Figure 3f).[32,37] These stretching-induced nanogaps and V-shaped-nanogrooves afford high-density hot-spots, which play an important role in confining incident photons as well as boosting Raman signals.

In order to evaluate the SERS capability of our polymer SPR film, a self-assembled monolayer of 4-methylbenzenethiol (4-MBT) is adsorbed on the polymer SPR film and then Raman signals of the probing molecules are obtained with a 514 nm laser as an excitation light source. Figure 4a compares the SERS performance of the PCL polymer film decorated with different thicknesses of Ag films before and after the stretching. It is found that when the thickness of Ag films reaches 25 nm, the SERS signal demonstrates the maximum enhancement after the stretching of our polymer SPR film from 4 to 10 cm. As can be seen, the SERS signals are very weak (only ~62 counts) for 1077 cm^{-1} peak before the stretching, which are attributed to the flat Ag film deposited on PCL polymer being able to offer a few hot-spots to enhance Raman signals. However, after the stretching, the SERS signals reach to ~630 counts, which are ~10 times larger. This phenomenon is because the stretched polymer SPR film leads to a much higher density of nanogaps among nanoparticles and nanogrooves, which function as plenty of hot-spots. These hot-spots with more intense local fields contribute to much better SERS performance. As the thickness of Ag film is increased, the period of the nanoribbon pattern becomes slightly larger from ~1 to 1.5 μm and the depth of nanogrooves turns to smaller, both of which result in the weaker intensity of SERS signals (Figure S5c–e). For the SERS performance of polymer SPR film without the stretching, when the thickness of Ag film is only 15 nm, noncontinuous Ag films are formed on the flexible substrate because of the Volmer–Werber growth mode, resulting in higher intensity of SERS signals than that of thicker Ag films.[38] However, at the thickness of 5 nm of Ag film, there are isolated Ag nanoparticles formed on the PCL polymer film. After the stretching, the distance between these adjacent nanoparticles become larger, leading to the weaker intensity of localized field among the nanogaps and then weaker SERS signals (Figure S8).

DOI: 10.1021/acsami.7b06669
ACS Appl. Mater. Interfaces 2017, 9, 26341–26349

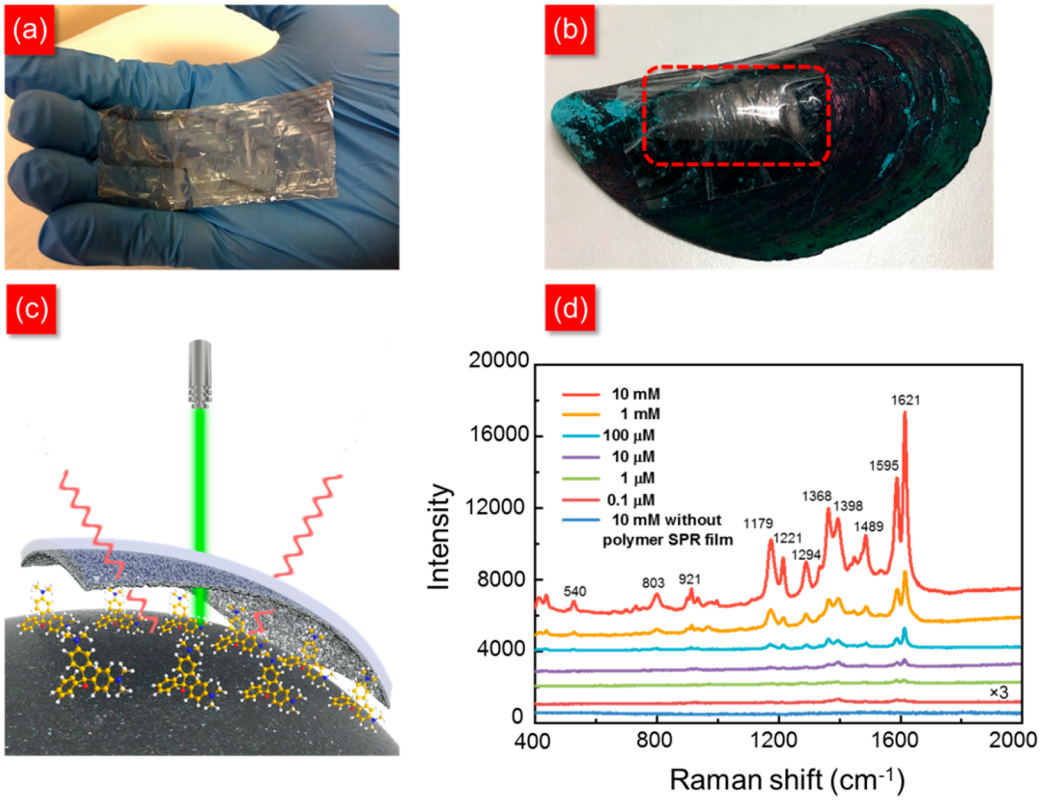

Figure 5. Demonstration of flexible polymer SPR film for practical SERS applications. (a) A photograph image of stretched polymer SPR film (8 cm × 4 cm). (b) A photograph image of polymer SPR film attached onto the green mussel surface contaminated by MG molecules. (c) Schematic diagram of contacting polymer SPR film onto the green mussel and collecting the SERS signals from the back side surface. (d) In-situ detection of MG molecules on the green mussel surface at various concentrations from 10 mM to 0.1 μM. The SERS spectra are obtained at the laser excitation wavelength of 514 nm, power 1.5 mW, acquisition time 10 s, and accumulation time 1.

In SERS applications, it is greatly significant to develop a universally reliable and stable system to generate reproducible SERS substrates with high uniformity from batch to batch. In such a system, the framework of SERS substrates' stability is highly crucial. Their property is required to endure the variance of the temperature. To demonstrate the stability of our polymer SPR film during the stretching (Figure 4b), extensive experiments at different temperatures are performed from room temperature (298 K) to 323 K. From the measured SERS spectra, it is observed that the performance of Raman signals has almost no degradation (9.62%), which shows the stable characteristic of the flexible SERS substrates. Furthermore, the signals' uniformity of the polymer SPR film is evaluated based on randomly extracting SERS signals over a large-area (4 cm × 4 cm) substrate. The spot-to-spot average relative standard deviation (RSD) of intensities at 1077 cm^{-1} is 6.48%, indicating excellent homogeneity and reproducibility of the flexible SERS film, which enables its potential applications in quantitative analyses (Figure 4c). The uniformity of our stretched polymer SPR film is superior to other flexible SERS substrates fabricated by lithographic methodologies (Table S1).[39−41] Meanwhile, via increasing the stretching ratio of the polymer SPR film, the intensity of SERS signals shows no obvious variation (6.47%) (Figure S10). It is found that the stretching ratio of our polymer SPR film can reach to ~650% because of the excellent ductility of PCL polymer film, which demonstrates its batch-fabrication capability to satisfy the requirements of low-cost, single-use, and easy-to-operate characteristics in lab-on-chip systems for POC applications.

The superiority of our polymer SPR film with good flexibility and transparency is able to serve as an effective tool for in situ, rapid and label-free identification of a wide variety of molecules. Different from the traditional rigid SERS substrates, the flexible plasmonic SERS film can be attached onto nonplanar surfaces and collect their Raman signals from the back side of the SPR film. We demonstrated this capability with the stretched Ag deposited polymer film as SERS substrates for in situ detection of malachite green (MG) molecules on green mussel surfaces (Figure 5b and c). Because of its functionality to control protozoan infections and fungal attacks associated with helminths on a variety of fish, MG has been widely applied in aquaculture and industries. However, it has the risk to pose potential problems on human health, such as organ damages and carcinogenic possibilities.[42] Before measuring the SERS signals, it should be noted that ~20 μL ethanol is dropped onto the flexible polymer SPR film to improve its conformal contact with the green mussel's surface and the adsorption of the MG molecules into the nanogaps as well as nanogrooves. As shown in Figure 5d, there are no Raman peaks observed after immersing the green mussel into 10 mM MG solution without attaching a polymer SPR film. While, with a stretched Ag-deposited polymer film seamlessly contacted with the non-planar surface of the green mussel, all characteristic Raman peaks of MG molecules are clearly distinguished, which are ascribed to the plenty of hot-spots formed on the stretched plasmonic polymer film, leading to huge enhancement of SERS signals. In particular, a tremendous enhancement of Raman shift at 1621 cm^{-1} is more evident associated with the vibration

DOI: 10.1021/acsami.7b06669
ACS Appl. Mater. Interfaces 2017, 9, 26341−26349

mode of ring C−C stretching, the intensity of which decreases gradually with lowering concentration of MG solutions. The detection limit can be down to as low as 0.1 μM. Although the detection limit of our result is not appreciable, this work aims to provide a facile approach to achieve cost-effective, large-area and homogeneous SERS film with the capability of mass production, which can be applied in resource-limited environments for POC diagnostics. This demonstrates a new noninvasive approach to realize in situ chemical identification on nonplanar surfaces and the ultrathin polymer SPR film is expected to access small corners of complex surface, such as carambola, which is very easy to hide and stay with residual pesticides.

Although stretching or cold-drawing of single polymer film has long been studied, where the mechanical properties of materials are reinforced with the tensile stress applying on the ductile polymer, the evolution of multimaterial composites via stretching still remains a virgin land.[43] Unprecedentedly, Shabahang et al. demonstrated highly sequential and controllable fragmentation of the cores to create uniform microrods by stretching multimaterial fiber.[30] However, it is still a long-standing challenge to create homogeneous structures at the nanoscale level through stretching the composite films. Our work based on longitudinally stretching Ag/PCL composites using the new biodegradable and biocompatible semicrystalline polymer can provide a new route to create uniform hybrid nanostructures. Such stretched flexible and productive polymer SPR film with high-density of hot-spots affords a new route for in situ detection of analytes residing on arbitrary topological surfaces, showing the potentials in environmental and food safety monitoring for POC diagnostics. Meanwhile, the stretching induced V-shaped nanogrooves can offer a variety of applications, such as efficient quantum emitter,[44] adiabatic nanofocusing,[45] nanophotonic circuitry[46] and nano-opto-mechanics.[47] Furthermore, our work based on stretching semicrystalline polymer composite can be extended toward other materials, such as gold (Au), alumina (Al), nickel (Ni), copper (Cu), or titanium (Ti). These unknown and intriguing morphological features are expected to be inspiring for other nanophotonic applications.

CONCLUSIONS

In conclusion, we have successfully realized biodegradable and flexible SERS substrates through a new environmentally friendly PCL polymer film as the building block. Via irreversibly and uniaxially stretching polymer SPR film, high-density of nanogaps and nanogrooves array are simply created, resulting in an order of magnitude (~10 times) enhancement of SERS signals than that of the unstretched polymer SPR film. Our flexible polymer SPR film can be intimately attached onto arbitrary shape surfaces of interest for in situ detection of analytes. Furthermore, our polymer SPR film exhibits highly stable and uniform SERS signals, making it feasible to generate reproducible SERS substrates from batch to batch. Meanwhile, the polymer SPR film can be extended further through developing hybrid Au/Ag/PCL or metal/insulator/metal/PCL systems to realize much higher performance of SERS enhancement. Our polymer SPR films with the characteristics of biodegradability and batch-fabrication have unprecedented opportunities to be integrated into portable Raman spectrometers for disposable applications as next-generation POC diagnostics, which are conceivable to penetrate into global markets and households in near future.

METHODS

Fabrication of Flexible SERS Substrates. The flexible PCL polymer film is cut into rectangular pieces at a dimension of 1 × 9 cm. To achieve different thicknesses of Ag film on the PCL polymer, a BOC Edwards AUTO 306 electron-beam evaporator is employed. The vacuum is pumped down to 4.0−5.0 × 10^{-6} Pa and the deposition rate is stabilized at 0.06 nm·s^{-1}. A quartz crystal oscillator is applied to monitor the film thickness. The deposition time determines the final thickness of Ag film. Then, Ag-coated PCL film is subjected to uniaxial stretching to various lengths under a constant velocity. The fabrication procedures of other metallic thin films, including Au, Ni, and Al, are the same. To evaluate the stability of PCL film at a higher temperature, a heating panel is used to elevate environmental temperature, which is monitored by a temperature measurement sensor.

Surface Morphology Characterization. Field-emission scanning electron microscope ((FESEM, JEOL FEG JSM 7001F) is used to characterize the morphologies of Ag-coated PCL films before and after the uniaxial stretching, operating at 5 kV at a working distance of 6−8 mm. The elements' distribution is analyzed by an energy-dispersive X-ray spectroscope (EDX, Oxford Instruments). In addition, a Tapping-mode Bruker SPM D3100 V atomic force microscope (AFM) is applied to reveal the 3D morphology of polymer SPR film after the stretching.

Optical Property Characterization. A CRAIC UV−vis−NIR microspectrometer QDI 2010 is applied to obtain the transmittance spectra from 300 to 900 nm of polymer films. The Fourier transform infrared (FT-IR) spectra of PCL polymer film are obtained by using a Shimadzu IRPrestige-21FT-IR spectrophotometer. The spectra are recorded using 50 scans at 4 cm^{-1} resolution from 400 to 2000 cm^{-1}. Furthermore, the plasmonic composite is investigated by X-ray diffraction (XRD, X'Pert PRO MRD) with CuKα radiation at a voltage of 40 kV and current of 40 mA. The scan range is from 10° to 30° at a step size of 0.02° and time per step of 10s. The optical constants of PCL polymer film are determined by using a variable angle spectroscopic ellipsometer at three different angles of incident light ranging from 65° to 75° at a step of 5°.

SERS Performance and Applications. To evaluate the SERS capability of the polymer SPR film before and after the stretching, the composite film is functionalized with a monolayer of 4-methylbenzenethiol (4-MBT).[48] The SERS film is then submerged inside a 4-MBT solution (10 mM) mixed with ethanol for 10 h and then rinsed inside an ethanol solution for 30 s, followed by nitrogen drying.[49,50] To demonstrate the SERS applications, green mussels purchased from a supermarket and then washed with deionized water are immersed in various concentrations of malachite green (MG) from 10 mM to 0.1 μM at a step of 10 for 8 h and dried at room temperature. Then, ~20 μL of ethanol is dropped onto the flexible SERS film to improve its conformal contact with the green mussel's surface and the adsorption of the MG molecules into the nanogaps, as well as nanogrooves. The Raman signals are then directly collected from the opposite side of the polymer SPR film. A Renishaw 2000 Raman imaging microscope equipped with a 514 nm continuous wave (CW) laser is used in the characterization. The Raman signals are collected through a 50× (NA = 0.8) microscope lens and detected by a thermoelectrically CCD array. The intensity of laser power is set as ~0.15 mW (evaluation of SERS performance) and 1.5 mW (demonstration of SERS applications) at an acquisition time of 10 s and accumulation time of 1.The spectra resolution is 1 cm^{-1}.

FDTD Simulation. To calculate the electric field distribution of uniaxially stretched polymer SPR film, numerical FDTD method from Lumerical Solutions, Inc. is applied to study the optical characteristic. A clear FESEM image of Ag coated polymer film after the stretching is imported into the FDTD software to create structures, followed by the scale definition. The polarized electromagnetic wave at the excitation wavelength of 514 nm with polarization along the uniaxially stretching direction is set to propagate normal to the structure surface. Perfectly matched layers (PML) are applied along z direction as boundary conditions to avoid the interference from the boundaries, while periodical boundary conditions (PBC) are applied in x and y

DOI: 10.1021/acsami.7b06669
ACS Appl. Mater. Interfaces 2017, 9, 26341−26349

directions. The electric field distributions are recorded by placing a 2D z-normal monitor in $x-y$ plane on the top surface of the structure. Similarly, to achieve the electric field distributions of the nanogroove, a 2D y-normal monitor in $x-z$ plane is employed. To achieve high resolution of electric field distribution, the mesh size region is set as $2.5 \times 2.5 \times 2.5$ nm and the monitor is placed inside the reduced mesh size region.

■ ASSOCIATED CONTENT

Supporting Information

The Supporting Information is available free of charge on the ACS Publications website at DOI: 10.1021/acsami.7b06669.

Surface morphology characterization; optical property characterization of PCL polymer film; EDX mapping to reveal Ag distribution; surface morphology of various metallic materials deposited on PCL film after the stretching; SEM images to support mechanisms' explanation; XRD and FTIR spectra of the stretched and unstretched PCL polymer films; thicknesses of Ag film's influence on SERS performance; uniformity demonstration; stretching ratio of polymer SPR film's influence on SERS performance; uniformity comparison of our polymer SPR film with reported flexible SERS substrates; Raman band assignment of 4-MBT and MG molecules (PDF)

Demonstration of stretching polymer SPR film (AVI)

■ AUTHOR INFORMATION

Corresponding Authors

*E-mail: ji_rong@dsi.a-star.edu.sg.

*E-mail: elehmh@nus.edu.sg.

ORCID

Kaichen Xu: 0000-0003-4957-3144

Ghim Wei Ho: 0000-0003-1276-0165

Minghui Hong: 0000-0001-7141-636X

Author Contributions

‡These authors contributed equally. K.C.X. performed the experiment, characterization, and simulation, as well as wrote the paper. C.F. T. and N. K. executed the 3D drawings. Z.Y.W. and M.H.H. conceived the design. R.J. participated in the characterizations. Z.Y.W., C.F.T., L.W.C., G.W.H., R.J., and M.H.H. discussed the results. All authors commented on the manuscript. M.H.H. proposed the original idea and supervised the project.

Notes

The authors declare no competing financial interest.

■ ACKNOWLEDGMENTS

This work is funded by A*STAR, SERC 2014 Public Sector Research Funding (PSF) Grant (SERC Project No. 1421200080). We thank Dr. Yu Yu Ko Hnin for XRD characterization. We also thank Mr. Hui Gao for processing the video. Mr. Goh Choon Hwa Ken is thanked for assisting the deposition of thin film. We also thank Mr. Yan Zhou for measuring the optical properties.

■ REFERENCES

(1) Boutry, C. M.; Nguyen, A.; Lawal, Q. O.; Chortos, A.; Rondeau - Gagné, S.; Bao, Z. A Sensitive and Biodegradable Pressure Sensor Array for Cardiovascular Monitoring. *Adv. Mater.* **2015**, *27*, 6954−6961.

(2) Zhong, J.; Zhang, Y.; Zhong, Q.; Hu, Q.; Hu, B.; Wang, Z. L.; Zhou, J. Fiber-based Generator for Wearable Electronics and Mobile Medication. *ACS Nano* **2014**, *8*, 6273−6280.

(3) Li, Y.; Luo, S.; Yang, M. C.; Liang, R.; Zeng, C. Poisson Ratio and Piezoresistive Sensing: A New Route to High-performance 3D Flexible and Stretchable Sensors of Multimodal Sensing Capability. *Adv. Funct. Mater.* **2016**, *26*, 2900−2908.

(4) Kaushik, A.; Kumar, R.; Arya, S. K.; Nair, M.; Malhotra, B.; Bhansali, S. Organic−inorganic Hybrid Nanocomposite-based Gas Sensors for Environmental Monitoring. *Chem. Rev.* **2015**, *115*, 4571−4606.

(5) Golightly, R. S.; Doering, W. E.; Natan, M. J. Surface-enhanced Raman Spectroscopy and Homeland Security: A Perfect Match? *ACS Nano* **2009**, *3*, 2859−2869.

(6) Irimia-Vladu, M. "Green" Electronics: Biodegradable and Biocompatible Materials and Devices for Sustainable Future. *Chem. Soc. Rev.* **2014**, *43*, 588−610.

(7) Cetin, A. E.; Coskun, A. F.; Galarreta, B. C.; Huang, M.; Herman, D.; Ozcan, A.; Altug, H. Handheld High-throughput Plasmonic Biosensor Using Computational on-chip Imaging. *Light: Sci. Appl.* **2014**, *3*, e122.

(8) Tokel, O.; Inci, F.; Demirci, U. Advances in Plasmonic Technologies for Point of Care Applications. *Chem. Rev.* **2014**, *114*, 5728−5752.

(9) Zhang, B.; Montgomery, M.; Chamberlain, M. D.; Ogawa, S.; Korolj, A.; Pahnke, A.; Wells, L. A.; Massé, S.; Kim, J.; Reis, L.; et al. Biodegradable Scaffold with Built-in Vasculature for Organ-on-a-chip Engineering and Direct Surgical Anastomosis. *Nat. Mater.* **2016**, *15*, 669−678.

(10) Kneipp, K.; Wang, Y.; Kneipp, H.; Perelman, L. T.; Itzkan, I.; Dasari, R. R.; Feld, M. S. Single Molecule Detection Using Surface-enhanced Raman Scattering (SERS). *Phys. Rev. Lett.* **1997**, *78*, 1667.

(11) Campion, A.; Kambhampati, P. Surface-enhanced Raman Scattering. *Chem. Soc. Rev.* **1998**, *27*, 241−250.

(12) Maier, S. A. *Plasmonics: Fundamentals and Applications*; Springer US: Boston, MA, 2007.

(13) Sharma, B.; Frontiera, R. R.; Henry, A.-I.; Ringe, E.; Van Duyne, R. P. SERS: Materials, Applications, and the Future. *Mater. Today* **2012**, *15*, 16−25.

(14) Jans, H.; Huo, Q. Gold Nanoparticle-enabled Biological and Chemical Detection and Analysis. *Chem. Soc. Rev.* **2012**, *41*, 2849−2866.

(15) Chan, S.; Kwon, S.; Koo, T. W.; Lee, L. P.; Berlin, A. A. Surface-enhanced Raman Scattering of Small Molecules from Silver-coated Silicon Nanopores. *Adv. Mater.* **2003**, *15*, 1595−1598.

(16) Polavarapu, L.; Liz-Marzán, L. M. Towards Low-cost Flexible Substrates for Nanoplasmonic Sensing. *Phys. Chem. Chem. Phys.* **2013**, *15*, 5288−5300.

(17) Liu, Q.; Wang, J.; Wang, B.; Li, Z.; Huang, H.; Li, C.; Yu, X.; Chu, P. K. Paper-based Plasmonic Platform for Sensitive, Noninvasive, and Rapid Cancer Screening. *Biosens. Bioelectron.* **2014**, *54*, 128−134.

(18) Chen, J.; Huang, Y.; Kannan, P.; Zhang, L.; Lin, Z.; Zhang, J.; Chen, T.; Guo, L. Flexible and Adhesive Surface Enhance Raman Scattering Active Tape for Rapid Detection of Pesticide Residues in Fruits and Vegetables. *Anal. Chem.* **2016**, *88*, 2149−2155.

(19) Liu, X.; Wang, J.; Tang, L.; Xie, L.; Ying, Y. Flexible Plasmonic Metasurfaces with User-designed Patterns for Molecular Sensing and Cryptography. *Adv. Funct. Mater.* **2016**, *26*, 5515−5523.

(20) Zheng, G.; Polavarapu, L.; Liz-Marzán, L. M.; Pastoriza-Santos, I.; Pérez-Juste, J. Gold Nanoparticle-loaded Filter Paper: A Recyclable Dip-catalyst for Real-time Reaction Monitoring by Surface Enhanced Raman Scattering. *Chem. Commun.* **2015**, *51*, 4572−4575.

(21) Mitomo, H.; Horie, K.; Matsuo, Y.; Niikura, K.; Tani, T.; Naya, M.; Ijiro, K. Active Gap SERS for the Sensitive Detection of Biomacromolecules with Plasmonic Nanostructures on Hydrogels. *Adv. Opt. Mater.* **2016**, *4*, 259−263.

(22) Kang, H.; Heo, C. J.; Jeon, H. C.; Lee, S. Y.; Yang, S. M. Durable Plasmonic Cap Arrays on Flexible Substrate with Real-time Optical

Tunability for High-fidelity SERS Devices. *ACS Appl. Mater. Interfaces* **2013**, *5*, 4569−4574.
(23) Kumar, S.; Lodhi, D. K.; Goel, P.; Neeti; Mishra, P.; Singh, J. P. A Facile Method for Fabrication of Buckled PDMS Silver Nanorod Arrays as Active 3D SERS Cages for Bacterial Sensing. *Chem. Commun.* **2015**, *51*, 12411−12414.
(24) Lamberti, A.; Virga, A.; Angelini, A.; Ricci, A.; Descrovi, E.; Cocuzza, M.; Giorgis, F. Metal−elastomer Nanostructures for Tunable SERS and Easy Microfluidic Integration. *RSC Adv.* **2015**, *5*, 4404−4410.
(25) Zuo, Z.; Zhu, K.; Gu, C.; Wen, Y.; Cui, G.; Qu, J. Transparent, Flexible Surface Enhanced Raman Scattering Substrates Based on Ag-coated Structured PET (Polyethylene Terephthalate) for in-situ Detection. *Appl. Surf. Sci.* **2016**, *379*, 66−72.
(26) Wu, W.; Liu, L.; Dai, Z.; Liu, J.; Yang, S.; Zhou, L.; Xiao, X.; Jiang, C.; Roy, V. A. Low-cost, Disposable, Flexible and Highly Reproducible Screen Printed SERS Substrates for the Detection of Various Chemicals. *Sci. Rep.* **2015**, *5*, 10208.
(27) Zhang, L.; Lang, X.; Hirata, A.; Chen, M. Wrinkled Nanoporous Gold Films with Ultrahigh Surface-enhanced Raman Scattering Enhancement. *ACS Nano* **2011**, *5*, 4407−4413.
(28) Qian, Y.; Zhang, X.; Xie, L.; Qi, D.; Chandran, B. K.; Chen, X.; Huang, W. Stretchable Organic Semiconductor Devices. *Adv. Mater.* **2016**, *28*, 9243−9265.
(29) Kim, J. Y.; Kim, H.; Kim, B. H.; Chang, T.; Lim, J.; Jin, H. M.; Mun, J. H.; Choi, Y. J.; Chung, K.; Shin, J.; et al. Highly Tunable Refractive Index Visible-light Metasurface from Block Copolymer Self-assembly. *Nat. Commun.* **2016**, *7*, 12911.
(30) Shabahang, S.; Tao, G.; Kaufman, J. J.; Qiao, Y.; Wei, L.; Bouchenot, T.; Gordon, A. P.; Fink, Y.; Bai, Y.; Hoy, R. S.; Abouraddy, A. F. Controlled Fragmentation of Multimaterial Fibres and Films via Polymer Cold-drawing. *Nature* **2016**, *534*, 529−533.
(31) Fang, T.; Li, W.; Tao, N.; Lu, K. Revealing Extraordinary Intrinsic Tensile Plasticity in Gradient Nano-grained Copper. *Science* **2011**, *331*, 1587−1590.
(32) Smith, C. L.; Thilsted, A. H.; Garcia-Ortiz, C. E.; Radko, I. P.; Marie, R.; Jeppesen, C.; Vannahme, C.; Bozhevolnyi, S. I.; Kristensen, A. Efficient Excitation of Channel Plasmons in Tailored, UV-lithography-defined V-grooves. *Nano Lett.* **2014**, *14*, 1659−1664.
(33) Wang, C.-Y.; Chen, H.-Y.; Sun, L.; Chen, W.-L.; Chang, Y.-M.; Ahn, H.; Li, X.; Gwo, S. Giant Colloidal Silver Crystals for Low-loss Linear and Nonlinear Plasmonics. *Nat. Commun.* **2015**, *6*, 7734.
(34) Lee, J.; Shim, W.; Lee, E.; Noh, J. S.; Lee, W. Highly Mobile Palladium Thin Films on an Elastomeric Substrate: Nanogap-based Hydrogen Gas Sensors. *Angew. Chem.* **2011**, *123*, 5413−5417.
(35) Chung, S.; Lee, J. H.; Moon, M. W.; Han, J.; Kamm, R. D. Non-lithographic Wrinkle Nanochannels for Protein Preconcentration. *Adv. Mater.* **2008**, *20*, 3011−3016.
(36) Lu, N.; Suo, Z.; Vlassak, J. J. The Effect of Film Thickness on the Failure Strain of Polymer-supported Metal Films. *Acta Mater.* **2010**, *58*, 1679−1687.
(37) Smith, C. L.; Stenger, N.; Kristensen, A.; Mortensen, N. A.; Bozhevolnyi, S. I. Gap and Channeled Plasmons in Tapered Grooves: A Review. *Nanoscale* **2015**, *7*, 9355−9386.
(38) Perumal, J.; Kong, K. V.; Dinish, U. S.; Bakker, R. M.; Olivo, M. Design and Fabrication of Random Silver Films as Substrate for SERS Based Nano-stress Sensing of Proteins. *RSC Adv.* **2014**, *4*, 12995−13000.
(39) Jeong, J. W.; Arnob, M. M. P.; Baek, K. M.; Lee, S. Y.; Shih, W. C.; Jung, Y. S. 3D Cross-point Plasmonic Nanoarchitectures Containing Dense and Regular Hot Spots for Surface-enhanced Raman Spectroscopy Analysis. *Adv. Mater.* **2016**, *28*, 8695−8704.
(40) Li, Z.; Meng, G.; Huang, Q.; Hu, X.; He, X.; Tang, H.; Wang, Z.; Li, F. Ag Nanoparticle-grafted PAN-nanohump Array Films with 3D High-density Hot Spots as Flexible and Reliable SERS Substrates. *Small* **2015**, *11*, 5452−5459.
(41) Chen, J.; Li, Y.; Huang, K.; Wang, P.; He, L.; Carter, K. R.; Nugen, S. R. Nanoimprinted Patterned Pillar Substrates for Surface-enhanced Raman Scattering Applications. *ACS Appl. Mater. Interfaces* **2015**, *7*, 22106−22113.
(42) Srivastava, S.; Sinha, R.; Roy, D. Toxicological Effects of Malachite Green. *Aquat. Toxicol.* **2004**, *66*, 319−329.
(43) Loos, J.; Schimanski, T.; Hofman, J.; Peijs, T.; Lemstra, P. Morphological Investigations of Polypropylene Single-fibre Reinforced Polypropylene Model Composites. *Polymer* **2001**, *42*, 3827−3834.
(44) Martín-Cano, D.; Martín-Moreno, L.; García-Vidal, F. J.; Moreno, E. Resonance Energy Transfer and Superradiance Mediated by Plasmonic Nanowaveguides. *Nano Lett.* **2010**, *10*, 3129−3134.
(45) Søndergaard, T.; Novikov, S. M.; Holmgaard, T.; Eriksen, R. L.; Beermann, J.; Han, Z.; Pedersen, K.; Bozhevolnyi, S. I. Plasmonic Black Gold by Adiabatic Nanofocusing and Absorption of Light in Ultra-sharp Convex Grooves. *Nat. Commun.* **2012**, *3*, 969.
(46) Burgos, S. P.; Lee, H. W.; Feigenbaum, E.; Briggs, R. M.; Atwater, H. A. Synthesis and Characterization of Plasmonic Resonant Guided Wave Networks. *Nano Lett.* **2014**, *14*, 3284−3292.
(47) Shalin, A. S.; Ginzburg, P.; Belov, P. A.; Kivshar, Y. S.; Zayats, A. V. Nano-opto-mechanical Effects in Plasmonic Waveguides. *Laser Photonics Rev.* **2014**, *8*, 131−136.
(48) Yang, J.; Li, J.; Gong, Q.; Teng, J.; Hong, M. High Aspect Ratio SiNW Arrays with Ag Nanoparticles Decoration for Strong SERS Detection. *Nanotechnology* **2014**, *25*, 465707−465713.
(49) Xu, K.; Zhang, C.; Zhou, R.; Ji, R.; Hong, M. Hybrid Micro/nano-structure Formation by Angular Laser Texturing of Si Surface for Surface Enhanced Raman Scattering. *Opt. Express* **2016**, *24*, 10352−10358.
(50) Xu, K.; Zhang, C.; Lu, T. H.; Wang, P.; Zhou, R.; Ji, R.; Hong, M. Hybrid Metal-insulator-metal Structures on Si Nanowires Array for Surface Enhanced Raman Scattering. *Opto-Electron. Eng.* **2017**, *44*, 185−191.

DOI: 10.1021/acsami.7b06669
ACS Appl. Mater. Interfaces 2017, 9, 26341−26349